Open Access Online Journal on Astronomy and Astrophysics

Acta Astrophysica Taurica

www.astrophysicatauricum.org

Acta Astrophys. Tau. 3(1), 44–47 (2022) doi:10.31059/aat.vol3.iss1.pp44-47

Determination of supermassive black hole spins in active galactic nuclei

A. Mikhailov

Radio Astrophysics Laboratory, Special Astrophysical Observatory of RAS, Nizhny Arkhyz, 369167, Russia
e-mail: mag10629@yandex.ru

Submitted on December 5, 2021

ABSTRACT

Abstract Black hole spin is a key to the relativistic jet generation. Existing models are based on the Blandford–Znajek and/or Blandford–Payne mechanisms. The jet power in these models is determined by the spin value, black hole mass, magnetic fields at the event horizon, and the accretion disc. Independent estimates of mass, jet power, and magnetic field give opportunity to constrain the supermassive black hole spin value. We present an application of this approach for supermassive black holes in different samples of active galactic nuclei (AGNs). We found that the assumption about equipartition between magnetic field energy density and accreting matter energy density is reasonable for the systems with thin accretion discs. The "mass-spin" diagrams were constructed for the samples of PG quasars and distant quasars at redshift $z \approx 4.8$ and demonstrated the flattening region at masses $M_{\rm BH} \approx 10^{8.5} M_{\odot}$. These diagrams can be used to study accretion onto supermassive black holes.

Key words: supermassive black hole, spin, magnetic field, relativistic jet

1 Introduction

A black hole can be characterized completely by two parameters: its mass $M_{\rm BH}$ and spin a. The spin is a dimensionless parameter and is determined by the angular momentum J of a black hole: $a = cJ/GM_{\rm BH}^2$ (Thorne, 1974). The spin can be changed by accretion, mergers, and the removal of the angular momentum by a jet (Fanidakis et al., 2011; Dotti et al., 2013; Volonteri et al., 2013; Dubois et al., 2014). Thus, determination of the spin allows us to study the history and characteristics of accretion into a black hole and investigate its significance for the generation of relativistic jets. To solve this problem, we have to construct a "mass–spin" diagram. The problem of determining the spin is more difficult compared to the problem of determining the mass of a black hole. The methods of X-Ray Reflection Spectroscopy (XRS) and Thermal Continuum Fitting (TCF) are currently more developed (see, e.g., reviews of Reynolds, 2014, 2019, 2021; Middleton, 2016). Both methods are based on the idea that the inner edge of the accretion disc is determined by the Inner Stable Circular Orbit (ISCO), which depends on the spin of a black hole. The accretion disc is thought to be geometrically thin with the Novikov–Thorne profile. Currently, the TCF method is applied mostly to the Galactic Black Holes (GBHs) because its application to Super Massive Black Holes (SMBHs) is difficult for some reasons. Thus, the majority of constraints on the spins of SMBHs are obtained with the XRS method. In this method the size of the ISCO (and hence the spin) is obtained from the shape of the Fe Kα 6.4 keV line profile. Qualitatively, the picture is like this: as the ISCO gets closer to the black hole, the Fe line manifests a wider profile. High-quality X-rays spectra are needed to successfully use the XRS method. Therefore, constraints of the SMBH spin have been obtained for approximately 40 objects because of the limited capabilities of modern instruments. These SMBHs are located mainly in nearby Seyfert 1 galaxies (Brenneman, 2013; Reynolds, 2021). We should note that the XRS method is biased towards SMBHs with higher spin values and is model dependent as well. Processing the same data set by different groups often leads to different results.

2 Method

The above mentioned reasons motivate us to search for other ways of constraining the spin value. An interesting possibility is the models of energy extraction by jets. These models are based on either Blandford–Znajek or Blandford–Payne mechanisms or both (so-called hybrid models, Meier, 1999; Garofalo et al., 2010). The approach was used in Daly (2009), Daly (2011), Daly and Sprinkle (2014). Jet power $L_{\rm j}$ is related to the mass of a SMBH $M_{\rm BH}$, magnetic field at the event horizon $B_{\rm H}$, and spin a: $L_{\rm j} \sim B_{\rm H}^2 M_{\rm BH}^2 a^2$. We can solve the equation for the spin if we know all the quantities in this formula. Jet power and mass can be found based on observational data. Unfortunately, there are no direct measurements of magnetic field values so far. Therefore, Daly used three assumptions about magnetic fields: 1) a constant value $B_{\rm H} = 10^4$ Gauss for all objects; 2) the Eddington limit value $B_{\rm Edd} \sim M_{\rm BH}^{-0.5}$; 3) a magnetic field proportional to the spin $B_{\rm H} \sim a$. As a result, constraints on the spin value were

obtained for more than hundred objects that have mostly FRII radio morphology.

Our approach is described in Mikhailov and Gnedin (2018), Mikhailov et al. (2019). Let us recall the main features. We used two hybrid models: above mentioned Meier's model (Meier, 1999) and the flux-trapping model (Garofalo, 2009; Garofalo et al., 2010). Within the framework of Meier's model we, unlike Daly, estimated the magnetic field based on the ratio between magnetic field energy density and accreting matter density: $B_{\rm H} = \frac{1}{R_{\rm H}}\sqrt{\frac{2\dot{M}c}{\beta}}$, where $R_{\rm H}$ is the radius of the event horizon, and $\dot{M}$ is the accretion rate. If we consider the situation when the magnetic field is generated by the accretion matter, then $\beta \geq 1$. Similarly, within the framework of the flux-trapping model, we estimated the magnetic field in the accretion disc $B_{\rm d}$ based on the ratio between magnetic field pressure and radiation pressure: $\frac{\beta_1 B_{\rm d}^2}{8\pi} = \frac{L_{\rm bol}}{4\pi c R_{\rm in}^2}$, where $R_{\rm in}$ is the inner radius of the accretion disc, and $L_{\rm bol}$ is the bolometric luminosity. As a result we obtained equations the left part of which is dependent on the spin and the right part contains jet power and bolometric luminosity of the accretion disc:

$$F(a) = \frac{|a|}{\sqrt{\varepsilon(a)}\left(1+\sqrt{1-a^2}\right)} = 1.77 \times \sqrt{\beta}\left(\frac{L_{\rm j}}{L_{\rm bol}}\right)^{1/2} \quad (1)$$

for Meier's model, where $\varepsilon(a)$ is the radiation efficiency of the accretion disc, and

$$X(a) = \frac{F(a)}{q^2(a)} = 16.48\beta_1\frac{L_{\rm j}}{L_{\rm bol}} \quad (2)$$

for the flux-trapping model, respectively.

The jet power and the bolometric luminosity can be found from observational data. We used an assumption about equipartition (β and β_1 are equal to one) for further calculations. This assumption is based on the hypothesis that the magnetic field is generated by accreting matter and therefore the energy density of the magnetic field cannot exceed the energy density of the matter. Thus, we can obtain a lower limit of the spin value by solving the corresponding equations.

3 Application

We applied our method to objects for which the spin value was obtained with the XRS method (Brenneman, 2013; Reynolds, 2021). The results are shown in Table 1. As we obtained a lower limit for the spin values, most of our results do not contradict the literature data. Objects from Brenneman (2013), Reynolds (2021) are mainly Seyfert 1 galaxies that have thin accretion discs. If we consider results obtained with the XRS method as true, then parameters β and β_1 should be bigger than one. In this case, the median values of β and β_1 are 1.5 and 1.8, respectively. Therefore, we conclude that the assumption about equipartition is reasonable, at least for the systems with thin accretion disks. Further, we consider the examples of using our method for different quasar samples.

Vestergaard and Peterson (2006) listed data about 70 PG quasars with redshifts from 0 to 0.5. We used their data

Table 1. Comparison with the XRS method.

Name	spin (XRS)	spin (M)	spin (FT)
MCG-6-30-15	$0.91^{+0.06}_{-0.07}$	$0.49^{+0.25}_{-0.17}$	$0.79^{+0.11}_{-0.12}$
Fairall 9	$0.52^{+0.19}_{-0.15}$	$0.88^{+0.12}_{-0.26}$	$0.93^{+0.05}_{-0.07}$
SWIFT J2127.4+5654	$0.72^{+0.14}_{-0.20}$	$0.61^{+0.29}_{-0.19}$	$0.85^{+0.08}_{-0.10}$
1 H0707-495	> 0.94	$0.38^{+0.21}_{-0.14}$	$0.72^{+0.12}_{-0.14}$
Mrk 79	> 0.50	$0.88^{+0.12}_{-0.26}$	$0.93^{+0.05}_{-0.07}$
Mrk 335	> 0.99	$0.56^{+0.27}_{-0.19}$	$0.83^{+0.09}_{-0.11}$
NGC 3783	> 0.88	$0.83^{+0.17}_{-0.24}$	$0.92^{+0.05}_{-0.08}$
Ark 120	> 0.85	$0.94^{+0.06}_{-0.27}$	$0.94^{+0.04}_{-0.07}$
3C 120	> 0.95	$0.52^{+0.27}_{-0.17}$	$0.81^{+0.10}_{-0.11}$
1 H0419-577	> 0.98	$0.35^{+0.21}_{-0.12}$	$0.70^{+0.13}_{-0.15}$
Ark 564	> 0.90	$0.70^{+0.30}_{-0.22}$	$0.88^{+0.07}_{-0.09}$
Mrk 110	> 0.99	$0.63^{+0.30}_{-0.20}$	$0.86^{+0.08}_{-0.10}$
Ton S180	> 0.98	$0.31^{+0.18}_{-0.12}$	$0.66^{+0.14}_{-0.16}$
RBS 1124	> 0.80	$0.64^{+0.31}_{-0.20}$	$0.86^{+0.08}_{-0.10}$
Mrk 359	$0.66^{+0.30}_{-0.54}$	$0.56^{+0.27}_{-0.19}$	$0.83^{+0.09}_{-0.11}$
Mrk 841	> 0.52	$0.48^{+0.24}_{-0.17}$	$0.79^{+0.10}_{-0.13}$
IRAS13224-3809	> 0.975	$0.42^{+0.22}_{-0.15}$	$0.75^{+0.11}_{-0.14}$
NGC 4051	> 0.99	> 0.73	$0.95^{+0.04}_{-0.06}$
NGC 1365	> 0.97	$0.83^{+0.17}_{-0.24}$	$0.92^{+0.05}_{-0.08}$

about SMBH masses and optical luminosity at 5100 Å to estimate the bolometric luminosity. The jet power was estimated according to the relation (Merloni and Heinz, 2007): $\log\frac{L_{\rm j}}{L_{\rm Edd}} = (0.49 \pm 0.07)\log\frac{L_{\rm bol}}{L_{\rm Edd}} - (0.78 \pm 0.36)$, where $L_{\rm Edd} \simeq 1.3 \times 10^{38} M_{\rm BH}/M_\odot$ [erg/s] is the Eddington luminosity. We have used this relation because it was established for the sample of nearby galaxies for which the jet power was estimated accurately enough by the cavities method. This method allows us to estimate the jet power based on the work needed to form emitting cavities (bubbles) (Allen et al., 2006; Rafferty et al., 2006). Moreover, we should note that the Merloni–Heinz relation was written in the form of dimensionless Eddington units. Currently, there is a lot of evidence that similar relations are true both for AGNs of different types and GBHs, so it extends to many magnitudes of jet power and bolometric luminosity (Daly et al., 2018). Thus, obtained estimates of jet powers and bolometric luminosities allow us to solve equations (1) and (2) and obtain lower-limit spin values. The "mass–spin" diagram is shown in Fig. 1. The asterisks indicate estimates within hybrid Meier's model, the triangles indicate estimates within the flux-trapping model. We note a trend of increasing the spin value with increasing mass, but this trend is replaced by flattening starting from masses $M_{\rm BH} \approx 2 \times 10^8 M_\odot$.

We used our method for a sample of distant quasars at redshift $z > 4$ in Mikhailov et al. (2019). The sample of 40 quasars at $z \approx 4.8$ were studied spectroscopically by Trakhtenbrot et al. (2011). From this paper we took the esti-

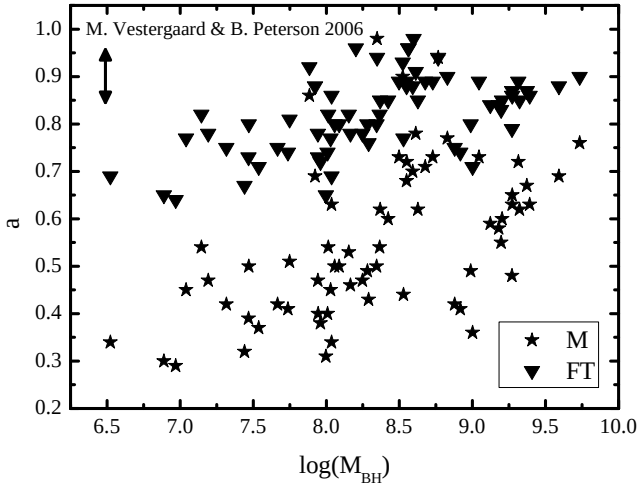

Fig. 1. The "mass–spin" diagram constructed for a sample of PG quasars. The data about SMBH masses and bolometric luminosities were taken from Vestergaard and Peterson (2006). The arrow denotes the mean error of spin estimation.

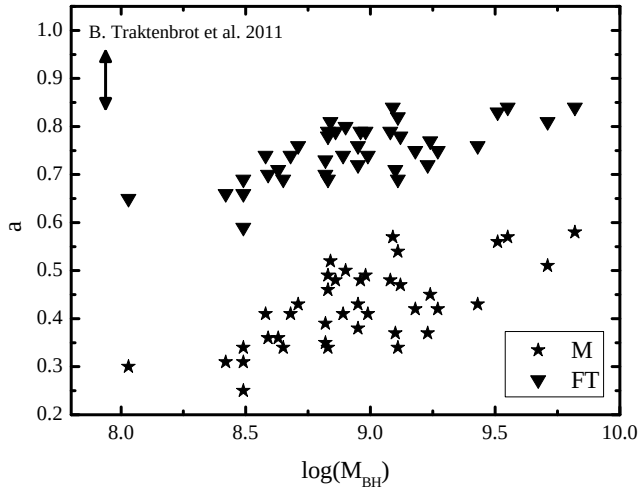

Fig. 2. The "mass–spin" diagram constructed for a sample of quasars at $z = 4.8$ (Mikhailov et al., 2019). The data about SMBH masses and bolometric luminosities were taken from Trakhtenbrot et al. (2011). The arrow denotes the mean error of spin estimation.

mates of SMBH masses and the data about optical luminosity which were used for calculations of bolometric luminosity. The jet power was estimated according to the Merloni–Heinz relation. The resulting "mass–spin" diagram is shown in Fig. 2. Designations are the same as in Fig. 1. The diagram is qualitatively similar to that obtained for PG quasars. We also note a trend of increasing the spin value with increasing mass, replaced then by flattening starting from masses $M_{\rm BH} \approx 6 \times 10^8 M_\odot$. Similar features are characteristic of the "mass–spin" diagrams obtained for other samples of quasars at high redshifts (Mikhailov et al., 2019).

Our method for constraining the spin value is necessarily dependent on accurate determination of the jet power and bolometric luminosity. There are a lot of empirical relations for estimating these quantities. In Mikhailov et al. (2019) we investigated how the results would change if different empirical relations were used. We concluded that despite changing spin values the shape of the relationship between spin and mass was generally constant.

Currently, there are many works dedicated to modeling SMBH evolution by mergers and accretion. "Mass–spin" diagrams are different depending on the characteristic of accretion: the prolonged or chaotic one (e.g., Fanidakis et al. 2011; Dotti et al. 2013). Therefore, it is possible to study the history and characteristic of the accretion onto SMBHs if we have a "mass–spin" diagram based on observational data.

4 Summary

Existing models for energy output from the rotation of a black hole by the way of relativistic jets allow us to obtain a spin value of SMBHs. However, there is currently no direct observational data about the magnetic field value near a black hole. For this reason we have used the assumption about equipartition for the systems with thin accretion discs. This assumption is supported if we consider the results of the spin value by the XRS method as true. We applied our approach for some quasar samples and found that the "mass–spin" diagrams have the flattening region at masses $M_{\rm BH} \approx 10^{8.5} M_\odot$. Such "mass–spin" diagrams can be used to study accretion onto SMBHs.

References

Allen S.W., Dunn R.J.H., Fabian A.C., Taylor G.B., Reynolds C.S., 2006. Mon. Not. Roy. Astron. Soc., vol. 372, no. 1, pp. 21–30.

Brenneman L., 2013. Measuring the Angular Momentum of Supermassive Black Holes. doi:10.1007/978-1-4614-7771-6.

Daly R.A., 2009. Astrophys. J. Lett., vol. 696, no. 1, pp. L32–L36.

Daly R.A., 2011. Mon. Not. Roy. Astron. Soc., vol. 414, no. 2, pp. 1253–1262.

Daly R.A., Sprinkle T.B., 2014. Mon. Not. Roy. Astron. Soc., vol. 438, no. 4, pp. 3233–3242.

Daly R.A., Stout D.A., Mysliwiec J.N., 2018. Astrophys. J., vol. 863, no. 2, 117.

Dotti M., Colpi M., Pallini S., Perego A., Volonteri M., 2013. Astrophys. J., vol. 762, no. 2, 68.

Dubois Y., Volonteri M., Silk J., 2014. Mon. Not. Roy. Astron. Soc., vol. 440, no. 2, pp. 1590–1606.

Fanidakis N., Baugh C.M., Benson A.J., et al., 2011. Mon. Not. Roy. Astron. Soc., vol. 410, no. 1, pp. 53–74.

Garofalo D., 2009. Astrophys. J., vol. 699, no. 1, pp. 400–408.

Garofalo D., Evans D.A., Sambruna R.M., 2010. Mon. Not. Roy. Astron. Soc., vol. 406, no. 2, pp. 975–986.

Meier D.L., 1999. Astrophys. J., vol. 522, no. 2, pp. 753–766.

Merloni A., Heinz S., 2007. Mon. Not. Roy. Astron. Soc., vol. 381, no. 2, pp. 589–601.

Middleton M., 2016. In C. Bambi (Ed.), Astrophysics of Black Holes: From Fundamental Aspects to Lat-

est Developments. Astrophysics and Space Science Library, vol. 440, p. 99. doi:10.1007/978-3-662-52859-4_3 (arXiv:1507.06153).
Mikhailov A.G., Gnedin Y.N., 2018. Astronomy Reports, vol. 62, no. 1, pp. 1–8.
Mikhailov A.G., Piotrovich M.Y., Buliga S.D., Natsvlishvili T.M., Gnedin Y.N., 2019. Astronomy Reports, vol. 63, no. 6, pp. 433–444.
Rafferty D.A., McNamara B.R., Nulsen P.E.J., Wise M.W., 2006. Astrophys. J., vol. 652, no. 1, pp. 216–231.
Reynolds C.S., 2014. Space Sci. Rev., vol. 183, no. 1-4, pp. 277–294.
Reynolds C.S., 2019. Nature Astronomy, vol. 3, pp. 41–47.
Reynolds C.S., 2021. Ann. Rev. Astron. Astrophys., vol. 59.
Thorne K.S., 1974. Astrophys. J., vol. 191, pp. 507–520.
Trakhtenbrot B., Netzer H., Lira P., Shemmer O., 2011. Astrophys. J., vol. 730, no. 1, 7.
Vestergaard M., Peterson B.M., 2006. Astrophys. J., vol. 641, no. 2, pp. 689–709.
Volonteri M., Sikora M., Lasota J.P., Merloni A., 2013. Astrophys. J., vol. 775, no. 2, 94.